JETIR.ORG ISSN: 2349-5162 | ESTD Year : 2014 | Monthly Issue
JOURNAL OF EMERGING TECHNOLOGIES AND INNOVATIVE RESEARCH (JETIR)
An International Scholarly Open Access, Peer-reviewed, Refereed Journal

Study of Atmosphere Potential Growth (PG) Variations at Local Climate Specification

Bharat Singh Jayant *, Sushanta Das

*Research Scholar, Department of Physics,
P. K. University, Shivpuri (M.P.) - 222001

Email: bharatsinghjayant@gmail.com

Abstract: The electrical system of the planet within the earth's atmosphere is referred to as atmospheric energy. It is enormously impact by extra-terrestrial or solar effects and these two components assume a significant part to frame earth atmospheric electric field potential. It is demonstrated that collocated atmospheric CO_2 data may be utilised as stratification proxies to detect circumstances that promote radon trapping and, as a result, change PG. PG was inhibited and GEC monitoring was impossible during steady nighttime conditions, when CO_2 rose steadily and at high quantities. A reverse connection between PG and CO_2 during the occurrence of a global signal might supplement the categorization of days as suitable or unsuitable in GEC monitoring.

1. Introduction: Climate refers to the short-term state of the atmosphere at a given time and place. Atmospheric pressure, temperature, solar radiations, relative humidity, precipitation, wind direction, and cloud cover are all important variables in determining this transient state of weather. As aggravated atmospheric conditions, extraordinary climate conditions or extreme meteorological unsettling influences may be considered [1]. These elements have such a great influence on the analysis of the electric field of the Earth's atmosphere. This part describes the observed atmosphere electric field influenced by certain forces that disrupt the climate. The atmospheric Global Electric Circuit (GEC) relationship with various metrological parameters can be detected through various climate change factors and it is criticality examine with multi tasking knowledge or by other effects. In any circumstance, there is indeed a significant scarcity of uncertain and constant measurements of atmospheric electric field strength properties that have probably contributed to a lack of information of GEC as well as its interaction local atmosphere [2]. At the surface, the ionospheric potential, vertical air-earth conduction flow, and ambient electric field are monitored. Last but not least, the predicted atmospheric parameters are known as Potential Growth (PG). PG is defined as the percentage of adjacent potential at height z to that height, PG = dV(z)/dz. During fair climatic times, PG is defined as optimistic and Ez = −PG is associated with the vertical component of the environmental

electric field. In any event, these impacts do not preclude, PG estimated under perturbed weather conditions from seeing GEC highlights on some occasions or by averaging, thereby making mainland locations similarly beneficial in the understanding of GEC. In addition of taking into account the fact that PG is responsible for the impacts of airborne pollution, space charges and common radioactivity at mainland locations, as recently alluded. Bits of information in a number of various wonders, periods, or times, such as explosions, air pollution, perceivability, limit layer observation, natural radioactivity measurement, and seismic tremors, can also be provided through its analysis at such destinations [3]. In comparison, in the discovery of significant meteorological phenomena, the ease of PG estimations, Parts of atmospheric electric field data in a number of various phenomena, processes, or occurrences, such as storms, air pollution, deceivability, maximum surface observation, typical radiation measurement, and seismic tremors, can also be provided through its analysis at such destinations. In comparison, in the discovery of significant meteorological phenomena, the utility of PG estimations, Carnegie twist is an ordinary technique for separating times where PG corresponds to worldwide GEC along with varieties including local variables on hourly, occasional, and annual time scales.

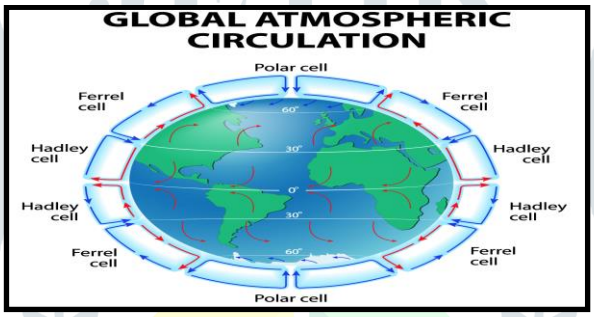

Fig. No.1 Atmospheric Global Circulation (https://www.internetgeography.net)

In this study, PG data is recorded from from June 2015 to May 2016 at station situated in the southern Balkans close to Xanthi, Greece. The nearest stations are Nagycenk, Hungary, a ways off 970 km and in Mitzpe Ramon, Israel, away from 1500 km. In addition to the integration of local PG climatology, the validity of the location in measuring GEC is investigated in this study. Furthermore, the possibility of deploying barometer estimates in assessing the step by step variation in PG is examined, and extraordinary concept is generated for the events when the enhanced description corresponds with the expected occurrences of the GEC signal [4]. Since this is a novel angle in the investigations of PG identified with atmospheric electric field, we intend to address this theme covers completely in future work. In contrast to the realistic atmosphere curves, the electric field diagrams recorded under disturbed atmospheric conditions provide an unusual contrast. Such curves could be considered almost as a context to correlate the normal atmosphere day with typical disturbances. The purpose of this chapter is just to develop up the ability to have these chronicles to forecast certain probable global electrical disaster [5].

This dataset contains electric field strength measurements for each sensor on the KSC Advanced Ground Dependent Field Mill network (AGBFM). The AGBFM network consists of 34 field mills, only 31 of which are operational as of 05/29/97. Such data were used in real time at KSC by the Launch Pad

Lightning Warning System (LPLWS). Each field mill detects the electrostatic field strength overhead of the system using stainless steel plates (stators) that are respectively shielded and exposed to the current atmospheric electric field by a grounded device.

An electric field metre (EFM Campbell Scientific Co., Utah, USA) has been installed since February 2011. An EFM sits in reverse on a 2-m tripod, surrounded by natural and man-made barriers such as trees, walls, poles, and cargo containers. However, since these obstacles are at least 30 m away and do not protrude higher than 18° above the horizon as seen from the ground at the EFM location, they really had no effect on the measurements .The PG values are symbolic if the distance between the measuring sensor and a field-distorting disturbance is five times the height of the disturbance or three times the height for thin obstacles such as pillars. These criteria are met by our platform; other stations have similar site characteristics [6] . Because the CS110 is a factory-calibrated field mill, no further tweaking is required for use .The calculation of a site-dependent correction coefficient, on the other hand as compared to an upward-facing flush-mounted installation; the elevated and reversed orientation of the EFM affects the effective gain. The coefficient was derived statistically based on the assumption that FW circumstances approximate to a theoretical PG value of 100 V m1. Select a set of reference FW days and divide the mean daily PG of each of these days by the usual FW–PG of 100 V m1 to get a number of daily determinations. Finally, an overall correction coefficient was calculated as the mean of the 50% of regular determinations across the median, and it was used to correct the PG data. Because of the severe statistical technique utilised to define the PG values, they are seen in relation to the conventional FW–PG relationship (100 V m1). The comparison FW days are chosen from datasets that include features from the FW standard definition, such as cloud cover less than 3/10 based on the MOD08 D3.051 cloud dataset with a resolution of 1°×1°, wind speed (WS) less than 3 on the Beaufort scale (4 ms^1), no precipitation events [7].

Disturbed weather (DW) days had at least one mean hour PG 0 V m1; negative PG values were attributed to local generators and were removed. The days that follow span the whole period, reducing any perceived seasonal bias. Since measurements were taken in all weather (AW) situations, like FW and DW, the EFM used two resolution modes. The resolution was 0.32 V m1 for measurements ranging from 0 to 2.2 kV m1, and 3.2 V m1 for measurements ranging from 2.2 to 22.3 kV m1.

Measurements of atmospheric electric field were made in conjunction with PG using an instrument fitted with a Gascard II Edinburgh Sensor (Schumann Analytics, Germany) from June 2011 to May 2012, spanning 150 days through the seasons. A reference analyzer was used to calibrate the CO_2 analyzer. Using a 0.52 l s1 pump, ambient air was continually sampled from the same 2 m height position where the PG was calculated. Since June 2011, commercially available sensors put at the same site as the EFM have provided standard meteorological characteristics such as WS/direction, temperature, relative humidity, pressure, and precipitation. Wind speed and direction were measured using a Wind Sentry Kit, which comprised a three-cup anemometer and a wind vane with 0.5 m/s and 5° accuracy, respectively. Temperature and relative humidity were determined using a 1.5 percent and 0.3-K precision thermometer/hygrometer, respectively (Model HygroClip S3; Rotronic Co., Switzerland). A 0.3-hPa

precision barometer pressure sensor was used to measure the pressure (Model PTB110; Vaisala Co., Finland). The precipitation was measured using a tipping bucket rain gauge (Model 52202; Young Co., Michigan, USA). From February to May 2012, two additional temperature (T) sensors (HOBO Pro v2 T/RH U23-001; Onset, Massachusetts, USA) with sun shields at 2% accuracy and 0.2% precision were placed at 2.5 and 1.5 m heights to give the vertical temperature gradient (DT). Except for the additional T sensors, which ran at f = 1/60 Hz, all sensors ran at 1 Hz, and data were recorded as 1-min means. After that, one-minute PG data were utilised to measure 10-minute data, which was subsequently used to generate hourly means. At regular intervals, the data collecting PC communicated with the National Institute of Standards and Technology (NIST) time server. Wherever the phrase "local time" (LT) appears in the book, it refers to Coordinated Universal Time (UTC) + 2; hence, no Daylight Saving Time was observed throughout the summer. The data provided here range from February 2011 to December 2014. Data from June 2011 to May 2012 were examined in greater depth. It is the first complete year of constant PG calculations and statistics for any of the other variables so far

2. Results and Discussion:

The analysis of the data collected on the mention days, and mean diurnal variations between perturbed weather conditions (PW)–potential gradient (PG) for each month of the period June 2015 to May 2016 at local climatic conditions.

a) The magnitude of the atmospheric electric field is highly sensitive to the smallest perturbations in the local climate variations. The data substantiates this premise as wave behavior shows extreme disturbance under the effect of the perturbed PG values.

b) Under the influence of extra terrestrial effect and perturbed weather conditions, atmospheric electric field undergo very sharp fluctuations with definitive sharp peaks and dips. A perfect correlation can be seen between the highest values of the PG and Atmospheric Electric field.

c) The extra terrestrial disturbances also affect the range in the magnitude of atmospheric electric field drastically. These waves oscillate with very sudden and sharp crest and troughs in extreme positive and extreme negative directions.

d) The most peculiar observation made in the behaviour of atmospheric electric field under the local climatic variation is the phenomena of wave inversion, which means the values of the magnitude of the atmospheric electric field falling in the negative direction, away from the earth with very high intensity which is never observed during the fair weather days. Such values fall as low as -20.70 kV/m.

e) The range of the magnitude of the atmospheric electric field during perturbed conditions is much broader as compared to those on fair weather days. The values of the atmospheric electric field tabulated in this chapter show a range of +20.897 to +0.25 kV/m (+20.647 kV/m) which is a much broader range as compared to the values obtained in fair weather days which fall in the rage +1.11 to +0.24 kV/m (+0.87 kV/m).

f) The comparative plotting of the values of the perturbed weather conditions (PW)–potential gradient (PG) with the magnitude of the atmospheric electric field depicts a very high correlation value as much as 0.605 which is a considerably high value.

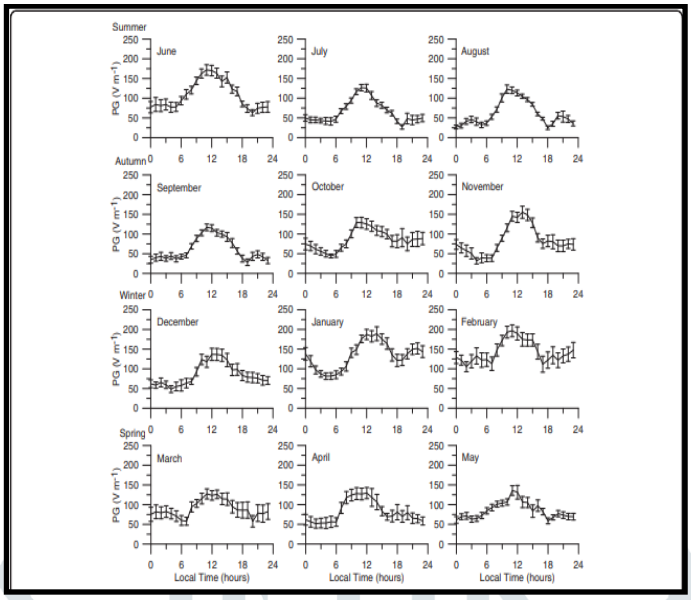

Figure No. 2 : Mean diurnal variations between perturbed weather conditions (PW)– For each month from June 2015 to May 2016, the potential gradient (PG) was calculated. Months are aligned according to the season. Error bars are displayed on the graph

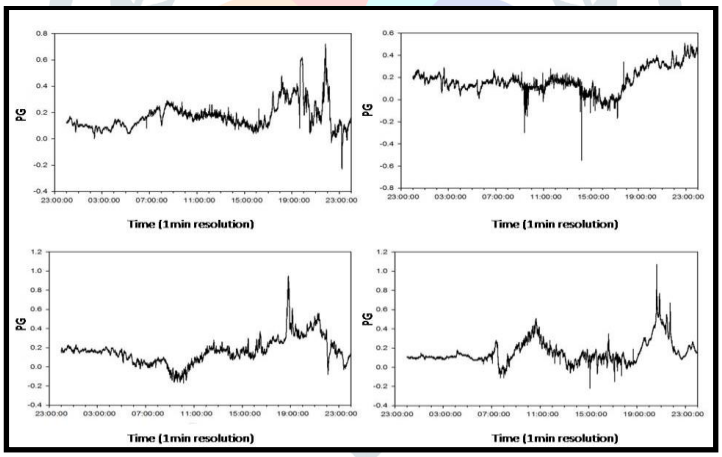

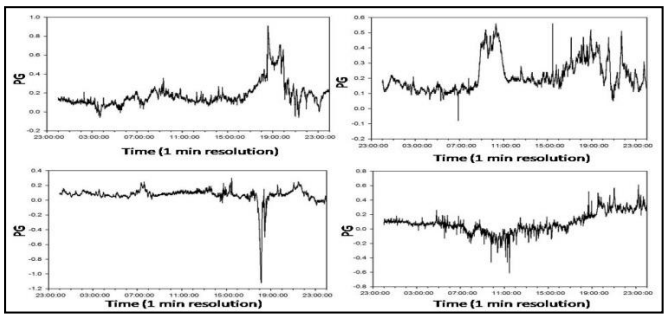

Hourly PG observations means the data resolution is 10 V m^{-1} for the period from June 2015 to May 2016 under local climatic condition. The vast majority of the values (93.6 %) was concentrated in the range of −200 to 350 V m^{-1} with all bins presenting a >0.1 % frequency of occurrence. The mean value and standard deviation (STD) were 66.24 and 649.90 V m−1, respectively. In Xanthi, the mean diurnal variation of FW–

PG followed the normal continental trend of the double peak. The main maximum occurred between 11:00 and 12:00 LT, while the secondary maximum occurred at 21:00 LT; the previous minima occurred at 5:00 and 18:00 LT, respectively [8-10]. The rising tendency of FW–PG throughout the early hours, followed by a main maximum around noon, is ascribed to local variables, including the "sunrise effect" and aerosols. This STD is unusually high due to the presence of disturbed circumstances, which can result in PG values of up to 15 kV m-1 or more, and the location has some of the highest levels documented in the southern Balkan Peninsula. We can see that the peak level is defined as the average number of days per year when thunder can be heard in a specific region and represents the probability of a thunderstorm occurring [11-12]. DW circumstances do not only include thunderstorms, but also incidents of charged clouds passing over the EFM and rain showers. Because of their strong electrostatic nature, these variables are thought to generate PG values that exceed the range of 200 V m-1 PG 350 V m-1, accounting for the remaining 6.4 percent of the entire distribution. The quantity of hourly values falling into the range 200 PG 0Vm1 is a substantial component of the distribution, accounting for 16.9 percent of the sample, in contrast to other locations where negative values are significantly less common. Because DW circumstances frequently produce PG reversal to negative values, these hours can be ascribed to them. The bulk of these values occur at night, independent of weather conditions; this suggests the presence of a local generator (local source of space charge production) powerful enough to produce enough negative space charge to cause PG reversal. Natural radioactivity is the most likely source of the event due to its timing and repetition [13-15]. Radioactive chemicals such as radon and its daughter products are confined near to the ground during nocturnal inversion, creating the reversed electrode effect and increasing negative space change density, which decreases PG values. The notion that natural radioactivity is a local generator that produces PG reversal is reinforced further by the station's position, which overlies granitic deposits and uranium ores with some of the greatest radon fluxes. Recent observations have verified this effect, which may also be responsible for enhanced conductivity around the research region. This component, together with the typically low aerosol concentrations exhibited by typical heavy pollution sources such as industry and big cities such as Athens, was responsible for a decreased PG mean value of 66.24 Vm^{-1}. Despite the apparent sub-hourly stability, the PG exhibits minor variations within each hour, primarily between 4 and 20 V m-1, indicating the impacts of changing local variables such as space charge and aerosols. So far, it is clear that the prevailing climatic circumstances during that hour (i.e., the presence of thunderstorms, the passing of charge clouds) and the presence of local generators have a substantial impact on both hourly PG values and their associated STDs (e.g., radon). These effects are of local origin and have the potential to totally conceal the PG response to GEC diurnal fluctuation. An FW–PG dataset was constructed to allow analysis of the diurnal and seasonal fluctuation of PG without the influence of DW situations and those with strong ionisation. Two basic criteria were utilised to choose the data for the FW set: 0 PG 350 V m 1 and PG-STD 100 V m 1. Negative PG readings were eliminated since they are related to either local sources (natural radioactivity) or DW circumstances. Furthermore, those with values greater than 350 V m-1, accounting for 2.7 percent of the distribution, were eliminated since they are associated with DW conditions or high aerosol concentration occurrences. The additional filter of PG-STD > 100 V m1 was used to exclude any

hourly values that subsequently fell within the range of 0–350 V m1 during the averaging process, despite being recorded under DW circumstances. The FW set had 78 percent of the total number of hourly means during the studied period. This large percentage of FW hours is advantageous for the station as compared to stations further north in Europe [16].

The approach of using PG statistics to determine the conditions under which it was collected and, ultimately, define an FW–PG set is beneficial, especially when cloud cover and local generator activity data are not available in high resolution and therefore the conventional FW definition may be used. In case for the Xanthi site the method are found for Marsta Observatory, Nagycenk Geophysical Observatory, are customized for diurnal and seasonal PG variation data. The double peak is followed at continental stations and is generally synchronized with local time and the intensity of local effects, while the GEC signal is not always apparent and averaging over one or several weeks is needed to be shown. The morning effect was thoroughly detailed, with a special emphasis on the PG response to positive space charge transpositions. The dawn effect was highlighted in the results, which included a charge reversal from negative to positive at the time of sunrise, corresponding with an increase in PG. The reason of solar heating, according to the convection process, is the breakdown of a shallow positively charged layer electrode layer that was built up over the night and overlies the very first decimeters of the ground. The dilution of the electrode layer shortly after dawn due to increased turbulence carries more and more positive charges over the EFM, eventually increasing PG values. Because of the downslope of a hilly terrain and the likelihood of valley or land wind closed circulation cells, the PG increase due to the sunrise effect may be amplified at Xanthi station. In such scenario, the electrode layer that developed on the mountain's surface throughout the night is likewise diluted after daylight, and the positive charges can be restored over the EFM via the returning cell circulation after being carried upslope. The importance of the dawn impact on the morning peak was also underlined in research for various stations, regardless of the site's type, such as normal continental, tropical continental, or island tropical. Aerosols have a direct influence on local conductivity because they function as recombination centres for the ions; at the same time, aerosols limit the mobility of the ions connected to them, lowering further conductivity. According to Ohm's law, a decrease in local conductivity, assuming a constant conduction current between the ionosphere and the earth, causes a rise in PG. Aerosols at the Xanthi site are predicted to have a higher arithmetic concentration at ground level throughout the morning to midday hours, resulting in higher PG values. The influence of aerosols on PG is exacerbated by the fact that the wind is generally blowing southeast to southwest at that time, transferring additional particles toward the EFM device. As a result, it is probable that at our station, the southern breezes and upwind road traffic, both of which are stronger around 9:00–10:00 LT, resulted in higher aerosol concentrations surrounding the station and followed the sunrise effect. This process may have resulted in a steadily growing influence on PG, which finally peaked at 11:00–12:00 LT. Thunderstorm activity in Asia, which was at its peak at the time, is another cause that might contribute to the morning growing trend of PG. Despite the fact that its contribution is deemed minor in comparison to the aforementioned elements, it is listed here as the only global component that may have an effect on the local

primary PG maximum. After the main high, PG began to fall and finally hit a low at 18:00 LT. This is due to the maximum of convective conditions in the late afternoon, which might induce dilution of aerosols near to the ground. Aerosols go upward, enabling ion concentrations to recover. Thus, according to Ohm's law under constant air–earth conduction current of PG = JZ/T, where JZ is the air–earth conduction current and T is total conductivity, local conductivity increases and PG decreases. Upward movement of aerosols progressively suppresses PG by lowering the conduction current. Because there is no mechanism for rapidly removing aerosols when they are high, columnar resistance rises, decreasing the air–earth conduction current (which generates PG force) and, as a result, PG. In comparison to the earlier data, when the comparable maximum occurred at 15:00 LT, a delay in columnar resistance maximising was seen at our location at 18:00 LT. We suspect that the delay is due to variations in advective circumstances at each location; greatest columnar resistance was found during low advection times. Both extremes, however, are subject to local influences that can either increase or suppress the global signal [17]. The previously optimum convective circumstances that resulted in a minimal PG value were gradually weakened, resulting in increasing aerosol concentration near to the ground and, as a result, increased PG. The progressive change to nighttime stratification might result in radon and its offspring being trapped, resulting in strong ionisation conditions and the formation of negative space charge (reversed electrode effect), which would finally inhibit PG. Negative space charge can also invert PG polarity; however, negative values were not taken into account. On certain days, the influence of radon during nighttime inversion might also alter the PG minimum (05:00 LT). The amount and timing of the impacts of local parameters on the global signal of PG are difficult to quantify; hence, measurements of other variables such as aerosol soundings, ground aerosols, conductivity, and radon are required. A comparison of the magnitude of the main peak with that of the Carnegie peak found a significant discrepancy, indicating that local effects dominate at Xanthi during the day considerably more than global influences. The diurnal fluctuation of AW–PG follows the same path as that of FW–PG, and it is held below the FW curve for the most of the day; this is consistent with PG behaviour at other locations. The predicted result was that DW circumstances were strongly recommended, and hourly variability was also obvious from the increased standard errors (SE), where SE = STD/n. Although it is not the same for all hours, it is sufficiently high to assure comparable PG values. The enhanced PG showed a pronounced intensity between 11:00 and 21:00 LT. During the same period, lightning activity is increased over Greece and Xanthi, the latter exhibiting the highest PG values. The perturbed condition coincides with the greatest divergence between the two curves, indicating the presence of non-PW. During some night hours, similar discrepancies between the two curves were also visible, however the non-PW circumstances here are more likely attributed to natural radioactivity. As a result, while the PW–PG typically followed a normal double-peak diurnal oscillation, the DW circumstances at our Xanthi site were sufficiently strong and frequent, leading the curve's minima and maxima to be much fuzzier than those of the FW–PG. Most of the days accompanied the general pattern described above, though in some cases, neither extreme was visible. During the warm months of June to October, the PG's primary maxima were at 10:00– 11:00 LT, but during the cold months of November to January, the maximum were transposed to 12:00–14:00 LT. The earlier onset of convective conditions during the warm

months is ascribed to this transposition, as is the earlier activation of the dawn effect. The remaining months, such as February and May, exhibited intermediate behaviour, with maxima occurring between 11:00 and 12:00 LT. The secondary maximum does not appear in every month, indicating the effect of local variables on PG during the global thunderstorm maximisation period. When a secondary maximum was seen in August, September, January, and May, it occurred within 1 hour of the Carnegie curve maximum at 19:00 UTC. The time variation might be related to seasonality of local variables like pollutants, regional changes in thunderstorm distribution that could disrupt the normal GEC cycle, or ionospheric disturbances. Finally, there was no seasonality in the two minima, which were located at 05:00 and 18:00 LT, respectively. Because the secondary peak occurs throughout the year, this effect is not purely seasonal. It is possible that it is the result of a combination of several contributing variables, including radon emanation, turbulence, and aerosol concentration and size distribution. Such assumptions, however, may only be hypothetical in the absence of pertinent evidence. Seasonal fluctuation in FW–PG observed from February 2011 to December 2014, with maxima (minima) during cold (warm) months. This fact, however, is inadequate to explain the higher aerosol concentrations close to the ground in winter because the primary heating sources in the area, notably the town of Xanthi and the village of Kimeria, are not upwind of the dominant wind directions found at the site. Furthermore, in Greece, columnar aerosol concentrations often peak in the spring/summer; however, other sources occur in the summer as well. In terms of air pollution, the boundary layer height (BLH) is the primary driver of aerosol concentrations near the ground. This arises on Mediterranean locations of the same latitude; the BLH during the summer may be up to ten times larger than that during the winter due to reduced convection during the winter. Large quantities of Aitkin nuclei efficiently lower the concentration of tiny ions that dominate the electrical conductivity of air, resulting in reduced local conductivity and, as a result, PG maximization. During the summer months, the boundary layer is significantly deeper than in the winter, scavenging aerosols that are close to the ground. Effects at the local against global levels Observing GEC from a single continental station is difficult because, as previously stated, local factors like as aerosols and space charge can totally obscure global changes. Local impacts, on the other hand, are either minimised at particular times or do not change much over time, allowing global signals to be observed. By comparing FW–PG with the Carnegie curve, an attempt is made to find similar periods for the Xanthi site. Because the GEC does not always follow a typical Carnegie curve due to factors such as local climate changes, rigid conclusions based on any sort of comparison with the Carnegie curve should be avoided. As long as the PG data are averaged over a sufficiently enough time, this curve is widely regarded as a fundamental tool for determining the periods in which PG represents GEC change. Furthermore, it has been observed that PG has a marginal latitudinal dependency, with the latitude impact influencing absolute PG levels. In the present study, the appropriate percentages of the means were used to compare local PG with the Carnegie curve. As a consequence, such impacts were no longer present. The FW–PG follows a similar path to global variation, with its minimum at 03:00 UTC and secondary maximum at 19:00 UTC coinciding with the Carnegie curve extremes; however, a disruption was seen during the development of the main maximum at 04:00–16:00 UTC. When the differences between the two cycles are estimated (DPG = FW–PG, Xanthi as

percentage of mean, the PG Carnegie curve as percentage of mean), the largest departure from the Carnegie curve occurs between 8:00 and 12:00 UTC, with a maximum divergence of 58 percent at 9:00 UTC. As previously mentioned, this is due to the dawn effect and aerosols. It might well result in an increase in negative space charge over the EFM, lowering the PG. With the completion of the shift to nocturnal stability, the variability of elements that might produce huge swings in PG, such as aerosols and radon, was decreased, allowing the PG to closely follow the Carnegie variation. DPG dropped below 25% between 21:00 and 04:00 UTC, and below 15% between 01:00–04:00 UTC, which were considered the best hours of the day for GEC observations at the Xanthi location. A same times (01:00– 04:00 UTC) have also been considered to be suitable for presenting GEC observations at Hungary's Nagycenk Geophysical Observatory continental station. To identify which months deviated from the Carnegie curve most little and thus are better suitable for GEC observation. This pattern is linked to atmospheric convection, which is stronger during the warm months. The atmosphere is more stable during the winter months, resulting in fewer diurnal fluctuations in aerosol and radon concentrations. As a result, the fluctuation of columnar resistance and local conductivity is decreased. Changes in the ionosphere composition induced by worldwide thunderstorm activity may also be to blame for the PG diurnal pattern. Cold months are similarly preferred in GEC data at other continental sites, where air convection seasonality is again thought to be the relevant process. The divergence from the typical trend of chilly months in November for the majority of the day might be due to increased atmospheric mixing or transient amplification of local variables such as aerosols and space charge. A PG values and local climatic conditions have been significant to global atmospheric electricity generation. Present studies have been performed on correlating local climatic elements with PG. By significance of the atmospheric electric field as stratification indication in the evaluation of PG is demonstrated here. Although the atmospheric electric field and the PG are two entirely separate variables, they are both impacted by convective circumstances; therefore a common factor is used to understand the PG diurnal cycle. For the period June 2011 to May 2012, the mean diurnal variation of common PG and atmospheric electric field values is presented. The PG values used in this study were obtained from the AW dataset, excluding days with rain and days with |PG| greater than 1 kV m1, the latter indicating the presence of heavily charged clouds. The previously mentioned values was excluded because they relate to disturbed situations that dominate PG variation with no influence. A comparison of the two cycles indicated an inverse connection between the PG and the atmospheric electric field (r 2 = 0.36, p value convection progressively increased, further decreasing the PG via an increase in columnar resistance and a consequent drop in the air–earth current). The latter mechanism, relating to PG, remained operational until 18:00 LT. The PW rose between 16:00 and 21:00 LT due to the progressive shift to nighttime stratification and the enforcement of atmospheric electric field sources. The PG approaches the secondary minimum around 18:00 LT and subsequently rises parallel to the CO_2 trend, displaying worldwide thunderstorm activity. The late afternoon and early evening hours, 18:00–00:00 LT, were particularly interesting. The global signal was predicted to peak at that time, and the concomitant evolution of stratification might have changed or totally obscured the planetary effect via radon trapping. In a 1-min time series for May 1–3, 2012, PG, CO_2, DT (DT = T2.5m T1.5m), and WS were studied as a case

study. It should be emphasised that cloud cover was 0.5 m1 during those days, which disrupted the very high stratification (DT > 0.5 °C) while concurrently lowering CO_2. Following that brief period, calm wind conditions resumed, resulting in increased stability (DT rises), which led CO_2 to rise and PG to fall. The previous evening, May 2, the stability continued with no significant disturbances until the GEC peak time of 21:00 LT, with the exception of a brief period soon after sunset when the stratification decreased significantly. During that brief amount of time, the PG started increasing in response to the GEC oscillation, but the rate of CO_2 rise was momentarily decreased. During this period, CO_2 continued to rise quickly and reach a peak, but PG fell dramatically, reversing the polarity and failing to display the worldwide signal. On the night of May 3, diurnal stratification started and persisted uninterrupted, causing a linear increase in CO_2 and totally obscuring the GEC. The PG remained low as well as even negative. The fluctuation of PG and CO_2 over those nights, particularly when the GEC signal was expected, shows that when CO_2 levels are stable and high, PG is suppressed and GEC detection is impossible. As a result, CO_2 fluctuations during stable nights may be used to supplementarily classify days as appropriate or unsuitable for GEC monitoring, given the absence of variables that could only affect PG, such as charged clouds overhead and aerosols. Furthermore, single-point CO_2 data may be used as proxies for turbulence and can provide information on the development of atmospheric electrical characteristics. In this technique, a positive correlation has been found between micrometeorology, atmospheric gases, and atmospheric electrical

4 Conclusions

The first four years of PG observations from a newly built rural station in Xanthi, Greece, are given in this study, from February 2011 to December 2014. The seasonal FW–PG fluctuation is typical for a Northern Hemisphere continental station, with maxima (minima) during cold (warm) months. The mean diurnal variation of FW–PG follows a typical continental double peak, with the primary maximum between 11:00 and 12:00 LT and the secondary maximum around 21:00 LT. The prominent peak was entirely linked to local factors, especially the sunrise effect and a spike in aerosol arithmetic concentration, the latter caused by the start of anthropogenic activities. The dawn effect is likely to be enforced at the Xanthi site since the station is positioned at the base of a hill, and local circulation effects occur after sunrise. Because its occurrence corresponds with the Carnegie curve maximum, the secondary peak might be attributed to global causes. However, it is also vulnerable to local impacts since the change from maximum of convective circumstances to nighttime stratification may result in an increase in aerosol concentration (trapped radon) acting positively (negatively) on FW–PG. FW–PG had its main maximum at 10:00–11:00 LT during the warm months of June to October, while the equivalent maxima were transposed to 12:00–14:00 LT during the cold months of November to January. The next months, from February to May, showed moderate behaviour, with maxima at 11:00–12:00 LT. Only in August, September, January, and May was the secondary maximum visible, and it occurred within 1 hour of the Carnegie curve maximum at 19:00 UTC. Although the AW–PG levels were typically lower, the diurnal fluctuation of AW–PG largely mirrored that of FW–PG. The significant thunderstorm activity at the location caused the AW–PG curve to

deviate from the FW–PG curve, as well as high AW–PG hourly variability. The nighttime FW–PG curve of Xanthi was highly linked with the conventional Carnegie curve. At the Xanthi location, the best hours for GEC observation were between 01:00 and 04:00 UTC, and cold months favoured global signatures more than warm months.

References:

1. A J Bennett and R G Harrison, Atmospheric electricity in different weather conditions, Royal meteorological Society, DOI: 1002/wea.97, 2007.
2. N. G. Kleimenova, O. V. Kozyreva, S. Michrowski, M. Kubicki, Effect of magnetic storms in variations in the atmospheric electric field at mid latitudes, Geomagnetism and Aeronomy, 48, 5,650 – 659, 2008.
3. M. J. Murphy, R. L. Holle and N. W. S. Demetriades, Cloud to Ground Lightning Warning using Electric Field Mill and Lightning Observations, 20th international Lightning Detection Conference Proceedings, 2008.
4. C. Demetrescu, and V. Dobrica, Signature of Hale and Gleissberg solar cycles in the geomagnetic activity, J. Geophys. Res., 113, A02103, doi:10.1029/2007JA012570, 2008.
5. K. E. Trenberth, J. T. Fasullo, and J. Kiehl. "Earth's global 2261 energy budget". Bull. Amer. Meteor. Soc. 90 , pp. 311–323. 2262 doi: 10.1175/2008BAMS2634.1. 2263, 2009.
6. D Jimenez, M Camargo, E Olark, I Santoyo, D Aranguran, J Herrena, E Perez, H Torres, M Salgado and G Gulrrers, Development of the natural laboratory for lightning induced voltages and atmospheric electricity study in La Palme, Columbia, 10th international symposium on lightning protection, Curitiba, 2009.
7. Macro A R Jusevicius, Armando Heilman, Cesar Beneti, Regional alert estimates and local variations in the atmospheric electric field- REMCEA system, X internation symposium on lightning protection, 2009.
8. Vical V Kumar, V Ramachandram, V Buadromo and J Prakash, surface fair weather potential gradient measurements from a small tropical island station Suva, Fiji, Earth planets space, 61,747-753, 2009.
9. A. Guha, B. K. De, S. Gurubaran, S. S. De and K. Jeeva. First results of fair-weather atmospheric electricity measurement in Northeast India. J. Earth Syst. Sci. 119, No. 2, pp. 221-228, April 2010.
10. C Pannelrselvam, C P Anil Kumar, Ajay Dhar, K U Nair, C Selvaraj, S Gurubaran and B M Pathan, Instrumentation for the surface measurements of atmospheric electrical parameters at Maitri, Antarctica: First result, Earth planets space, 62,545-549, 2010.
11. S D Pawar, P Murugavel and V Gopalakrishnan, Anomalous electri field changes and high flash rate beneath a thunderstorm in northeast India, J Earth Syst. Sci. 119, No. 5, pp.617-625, 2010.
12. R Giles Harrison and Ilya Usoskin, Solar modulation in surface atmospheric electricity, Journal of atmospheric and solar terrestrial physics 72, 176-182, 2010.
13. Wei He, Hong Jian Liu, Ba Lin Yu, Xiao Chang Liang and You Ju Liu, Application of ground electric field information in lightning forecast, Future Intelligent Information systems, LNEE 86, pp.577-583, 2011.

14. Pizzo, V., Millward, G., Parsons, A., Biesecker, D., Hill, S. and Odstrcil, D., Space Weather, 9, S03004., 2011.

15. Ferro, Macro Antonio, de Silva, Lightning Risk Warning Based on Atmospheric Electric Field Measurement in Brazil, J. of Aerospace Technological Management. Vol. 3 ISSN 1984-9648, 2011.

16. Herbert KBH, John Canton, Pioneer investigator of atmospheric electricity, Weather 52: 286-290, https://doi.org/10.1002/j.1477-8696.1997.tb06326.x, 2012.

17. H G Silva, R Conceicao, M Melgeo, K Nicoll, P B Mendes, M Tlemcani, A H Reis and R G Harrison, Atmospheric electri field measurement in urban environment and the pollutant aerosol weekly dependence, Environmental research letters, 2014.